L-3-[^{123}I]Iodo-α-Methyl-Tyrosine SPECT in Non–Small Cell Lung Cancer: Preliminary Observations

Pieter L. Jager, Harry J.M. Groen, Annija van der Leest, John W.G. van Putten, Remge M. Pieterman, Elisabeth G.E. de Vries, and D. Albertus Piers

PET Center and Departments of Nuclear Medicine, Pulmonary Diseases, Radiotherapy, and Medical Oncology, University Hospital Groningen, Groningen, The Netherlands

L-3-[^{123}I]iodo-α-methyl-tyrosine (IMT) is a modified amino acid that is avidly taken up by many tumors. Uptake is based on the increased transmembrane transport of amino acids in malignancies. IMT is the only amino acid tracer suitable for SPECT. The aim of this study was to determine the feasibility of IMT SPECT in the detection, staging, and treatment evaluation of non–small cell lung cancer. **Methods:** We evaluated 44 IMT SPECT studies in 17 patients with histologically proven non–small cell lung cancer, stage III. IMT SPECT and planar imaging of the chest was performed before, 2 wk after, and 3 mo after 60 Gy radiotherapy. Staging was based on the findings of bronchoscopy, chest CT, mediastinoscopy, or explorative thoracotomy. After radiotherapy, CT and bronchoscopy were repeated to assess tumor response. **Results:** In 15 of 16 evaluable primary tumors, avid IMT uptake was present (sensitivity, 94%), with a mean (±SD) tumor-to-background ratio (T/B) of 2.95 ± 0.78 (range, 1.7–4.9). In 12 of 14 patients (86%) with mediastinal involvement, IMT SPECT detected one or more mediastinal metastases. However, only 13 of 20 mediastinal metastases were detected in lesion analysis (lesion-based sensitivity, 65%). For lesions < 2 cm in diameter, sensitivity was 42%. FDG PET (available for 5 patients) detected more known and unknown lesions than did IMT SPECT. After radiotherapy, T/B had fallen to 1.84 ± 0.29 ($P < 0.001$ vs. baseline), and 3 mo later to 1.61 ± 0.41 (not statistically significant vs. second study). Considerable nonspecific uptake was found in irradiated normal lung tissue (mean ratio to nonirradiated tissue, 1.79 ± 0.53), persisting for > 3 mo. No relationship was observed between various IMT uptake parameters and the presence of residual viable tumor tissue or survival. **Conclusion:** IMT SPECT has a high sensitivity for the detection of primary non–small cell lung cancer. Although patient-based sensitivity in detecting mediastinal spread was adequate, sensitivity for individual lesions, especially for small metastases (<2 cm in diameter) was too low to be clinically helpful. Radiotherapy caused considerable nonspecific IMT uptake, which also limits applicability in evaluating the results of treatment.

Key Words: ^{123}I-methyl-tyrosine; lung cancer; mediastinal staging; SPECT; treatment evaluation

J Nucl Med 2001; 42:579–585

Received Jul. 10, 2000; revision accepted Nov. 9, 2000.

For correspondence or reprints contact: Pieter L. Jager, MD, Department of Nuclear Medicine, University Hospital Groningen, P.O. Box 30001, 9700 RB Groningen, The Netherlands.

Metabolic imaging of non–small cell lung cancer is gaining clinical interest. In contrast to anatomic imaging methods such as CT, imaging methods such as SPECT and PET visualize metabolic activity within tumor lesions. This metabolic information can be used for characterization of tumor lesions, primary staging, and evaluation of treatment. The most prominent example of these methods is PET using ^{18}F-FDG (*1–4*). However, PET has several disadvantages: its availability is still limited, costs are high, and the tracer FDG is also taken up by inflammatory lesions (*5*).

Radiolabeled amino acids may be an interesting alternative in the metabolic imaging of lung cancer. Because amino acid uptake in inflammatory lesions is less prominent than FDG uptake, these tracers may be more tumor specific (*6,7*). This tumor specificity may especially be helpful in evaluation of residual tumor activity after treatment or in detection of recurrence.

The radiolabeled amino acid L-3-[^{123}I]iodo-α-methyl-tyrosine (IMT) has been introduced for brain tumor imaging but is also taken up by many other tumors (*8,9*). Uptake is based on the increased transport of amino acids, present in nearly all cancer cells (*10–12*). Uptake appears to be related to tumor proliferation, as shown in vivo in brain and soft-tissue tumors and in vitro in tumor cell lines (*13,14*). Application of IMT in lung cancer patients has not, to our knowledge, been studied. The ^{123}I radiolabel makes the tracer suitable for SPECT. In comparison with PET, use of SPECT is advantageous because of better availability and lower costs but disadvantageous with respect to image resolution. The aim of this study was to investigate the feasibility of IMT SPECT in detection, primary staging, and evaluation of radiotherapeutic treatment in patients with non–small cell lung cancer.

MATERIALS AND METHODS

Patients

Patients with histologically proven non–small cell lung cancer were included in the study between September 1997 and October 1998. We selected consecutive patients with inoperable or unre-

sectable stage IIIA or IIIB cancer who were scheduled for radiotherapy. The patients were imaged three times: before radiotherapy, 1–2 wk after the end of radiotherapy, and 3 mo after the second study. Written informed consent was obtained from all patients before inclusion. The study was approved by the medical ethics committee of Groningen University Hospital.

Mediastinal lymph node staging was based on histologic or cytologic information obtained during endobronchial carinal puncture, cervical mediastinoscopy, or explorative thoracotomy. When direct mediastinal tumor involvement (T4 tumor) was observed, the disease was not further staged using invasive procedures. In all other cases, the mediastinal status was based on histologic or cytologic information.

All patients were treated with radiotherapy (60 Gy, in 30 daily fractions) of the primary tumor and mediastinal metastases. Assessment of response was based on measurement of remaining tumor size on CT images obtained within 2 wk after the end of radiotherapy and on repeated bronchoscopy with biopsy when possible. Patients were followed up until June 2000. The duration of survival and the cause of death were recorded.

Chest CT

CT of the chest and upper abdomen was performed with a Tomoscan SR7000 (120 kV, 125 mA; Philips, Eindhoven, The Netherlands) with a slice thickness of 5–10 mm. Scanning time was 1 s per slice. Two hundred milliliters of contrast medium (Omnipaque; Nycomed, Buckinghamshire, U.K.) were administered intravenously (1.5 mL/sec). CT images were interpreted independently by a radiologist and a pulmonologist not aware of IMT or PET findings. Tumor size was determined by measuring the two largest perpendicular dimensions on a representative transverse slice. Mediastinal lymph nodes were divided into two categories: nodes with a short-axis diameter < 1 cm were interpreted as benign (negative), nodes ≥ 1 cm were considered metastases (positive).

IMT SPECT

Synthesis of IMT was performed as previously described (*9*). After at least a 5-h fast, SPECT of the chest was performed 15 min after the intravenous injection of 250–300 MBq IMT using a large-field-of-view double-head gamma camera (MULTISPECT 2; Siemens Inc., Hoffman Estates, IL) with a medium-energy all-purpose collimator (64 views, 30 s per view). Additional planar spot views were acquired for 10 min. Transaxial tomograms were reconstructed using filtered backprojection with a Butterworth filter (sixth order; cutoff, 0.275 Nyquist). System resolution was 12 mm full width at half maximum at a 10-cm distance.

All images were interpreted from a computer monitor by an experienced nuclear medicine physician unaware of other imaging information. Planar images were qualitatively analyzed using a simple scoring system: + = uptake just above background uptake, ++ = uptake higher than background uptake, and +++ = uptake much higher than background uptake. Areas of abnormal IMT uptake were defined as areas with clearly increased SPECT uptake compared with normal background uptake (*9*).

Semiquantitative measurements of IMT uptake were performed by defining regions of interest (ROIs) around the lesion under study. These regions were drawn on transverse SPECT slices with maximum tumor visibility and were drawn in a standardized fashion at 80% of the maximum pixel value in the lesion. A background ROI was drawn in contralateral normal lung tissue, and from the uptake intensity (counts per pixel) in both ROIs the tumor-to-background ratio (T/B) was calculated. T/Bs were calculated before and after radiotherapy on corresponding transverse SPECT slices. After radiotherapy, ROIs were identically drawn at 80% of the maximum pixel value of the remaining tumor, which usually had shrunk through the irradiation. Radiotherapy-induced volume changes were not considered in this way, and T/Bs after radiotherapy thus represent tracer uptake density in the remaining tumor volume. To study the effect of radiotherapy on normal lung tissue, an additional ROI was drawn in normal lung tissue that had been included in the radiotherapy field. In this way, a radiated-to-nonirradiated ratio (R/NR) was calculated.

Statistics

Paired Student *t* tests were used to compare T/Bs and R/NRs at various times, because differences did not deviate from normal distribution, as evidenced by Kolmogorov-Smirnov tests. One-sample *t* tests were used to compare R/NRs with the expected value 1. Mann-Whitney U tests were used to compare IMT uptake data in patients with positive versus negative biopsy or mediastinal status. Spearman rank correlation was used to compare tumor area reduction with IMT T/B reduction. Two-tailed probability values < 0.05 were considered significant.

RESULTS

Patients

Seventeen patients underwent an IMT SPECT study before radiotherapy (Table 1). In patient 13, the primary tumor had been removed for diagnostic purposes, leaving 16 primary tumors evaluable. The maximal tumor diameter was between 1.5 and 7 cm, with a mean of 4.5 cm. In 4 patients, an explorative thoracotomy had been performed 20, 32, 44, or 50 d before the IMT study. Five patients had also undergone FDG PET.

The mediastinum was positive for lymph node metastases in 14 (82%) of the 17 patients using the staging method described above. Six patients had direct tumor involvement of the mediastinum (T4). In 11 patients, CT of the chest revealed one or more mediastinal lymph nodes ≥ 1 cm in diameter; in the other 6 patients mediastinal lymph nodes were either absent or <1 cm in diameter. The patient-based sensitivity of CT for the detection of mediastinal metastases therefore amounted to 79% (11/14). The 14 patients with mediastinal metastases had a total of 20 metastatic locations, 8 of which contained metastases between 2 and 4 cm in diameter. Twelve locations contained metastases < 2 cm in diameter, of which 6 were <1 cm.

First IMT SPECT (Tumor Detection and Mediastinal Staging)

IMT SPECT clearly depicted 15 of the 16 evaluable primary tumors (94%). Examples are presented in Figures 1 and 2. The only tumor that was not detected was the smallest in this study and was 1.5 cm in diameter (patient 16 in Table 1). Tumors were usually already visible on planar images, but SPECT greatly increased visibility and improved localization. IMT tumor uptake was high, with a mean T/B of 3.0 ± 1.0 (SD) and a range of 1.7–6.1 (Table 1).

In 12 of the 14 patients with mediastinal metastases, IMT SPECT detected abnormal uptake in the mediastinum,

TABLE 1
Patients, Primary Tumors, and IMT Uptake

Patient no.	Sex	Age (y)	Tumor histology	Size (cm)	Location	Tumor stage	Nodal stage	Clinical stage	IMT uptake, planar*	T/B SPECT
1	M	66	Squamous	2	RUL	T3	N2	IIIA	+++	3.0
2	M	52	Squamous	6	RML	T3	N2	IIIA	+++	6.1
3	M	58	Large cell	4	RML	T2	N2	IIIA	+	1.8
4	M	63	Squamous	6	RUL	T3	N2	IIIB	+++	3.4
5	F	55	Adenous	5	RUL	T4	N0	IIIB	++	2.9
6	F	68	Squamous	5	RML	T2	N2	IIIA	++	2.6
7	M	42	Squamous	3	LUL	T3	N2	IIIB	++	3.1
8	M	67	Squamous	5	LUL	T4	N0	IIIB	+++	3.4
9	M	71	Squamous	6	RUL	T4	N2	IIIB	+++	3.1
10	F	70	Adenous	4	RLL	T3	N2	IIIB	++	3.0
11	M	56	Squamous	4	RLL	T4	N2	IIIB	+	1.8
12	M	69	Large cell	5	RUL	T4	N2	IIIB	+++	3.6
13	M	50	Excised	—	LLL	—	N2	IIIB	−	
14	F	69	Adenous	7	RUL	T4	N2	IIIB	++	3.2
15	M	41	Large cell	5	RUL	T2	N2	IIIB	++	2.7
16	F	62	Squamous	1.5	LUL	T1	N3	IIIB	−	
17	F	74	Squamous	4	LUL	T3	N0	IIIB	+++	3.8

*− = not visible; + = uptake just above background; ++ = uptake higher than background; +++ = uptake much higher than background.

RUL = right upper lobe; RML = right middle lobe; LUL = left upper lobe; RLL = right lower lobe; LLL = left lower lobe.

yielding a (patient-based) sensitivity of 86% (Fig. 2B). One patient (patient 4) had multiple small mediastinal metastases (1–2 cm in diameter) that were not visible on the IMT images. In the other patient (patient 11), a 2-cm hilar/paratracheal lesion was not detected, presumably because of low uptake. No findings were false-positive.

When individual mediastinal lesions were analyzed, IMT SPECT detected 13 of the 20 metastatic locations (overall lesion-based sensitivity, 65%). All 8 locations containing metastases $>$ 2 cm in diameter were detected. However, only 5 of the 12 locations containing metastases $\leq$ 2 cm were detected (small-lesion sensitivity, 42%). Because of limited resolution, metastatic locations could not always be clearly separated. For example, patient 12 had a metastasis of 2-cm diameter in the transition zone between the hilar and paratracheal region and an additional carinal metastasis. Although increased uptake was found in the entire perihilar region, the two histologically confirmed metastases could not be visualized separately on the IMT SPECT images.

In one patient, IMT SPECT showed clearly increased uptake in an unexpected supraclavicular lesion. This finding was originally considered to be false-positive, because the lesion had not been found during staging, but 3 mo later (after radiotherapy, not including the supraclavicular area) a palpable metastatic node was found in this location. Apart from this instance, no other unexpected abnormalities were found, in particular no distant metastases.

In five patients, FDG PET had also been performed, and the results were compared with IMT SPECT. All primary tumors were also visualized using PET. In one patient (patient 11), IMT did not detect a 2-cm mediastinal lymph node, which was positive on PET. However, PET showed

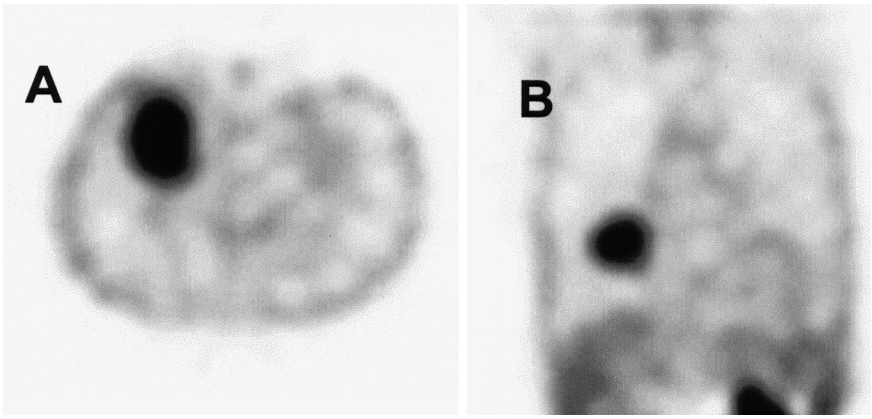

FIGURE 1. Transverse (A) and coronal (B) SPECT slices through squamous cell lung carcinoma in right middle lobe (patient 2) show intense IMT uptake.

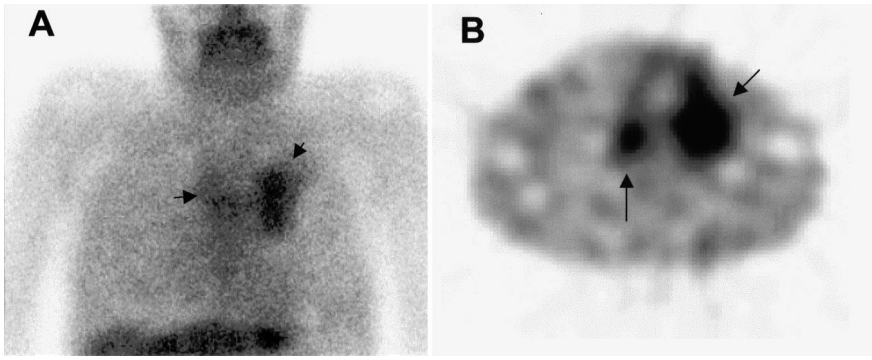

FIGURE 2. (A) IMT planar image of chest shows uptake in primary squamous cell carcinoma in left upper lobe and uptake in mediastinum (arrows). Minor, presumably bone marrow, uptake in sternum overlies mediastinal lesion (B). Transverse SPECT slice from same patient shows better delineation of primary tumor in left upper lobe and clear mediastinal metastasis (arrows).

two false-positive mediastinal locations (1.5 cm) that were correctly negative on IMT SPECT. In two other patients, PET detected unexpected small, distant metastases; one in bone (confirmed with bone scintigraphy; more bone metastases developed during follow-up) and one intrapulmonary (clearly grew during follow-up). As expected, image quality, anatomic resolution, and lesion-to-background activity for PET were superior to those for IMT SPECT (Fig. 3).

Second IMT SPECT (After Radiotherapy)

The second IMT SPECT examination, shortly after the end of radiotherapy, was performed on 14 patients. In 3 patients, scanning was not performed after treatment because radiotherapy had been canceled. In 1 of these patients, the disease had progressed shortly after the start of treatment; the other 2 patients had died. In patient 13, whose primary tumor had been removed for diagnostic purposes, a 3-cm mediastinal metastasis had been irradiated. This lesion was used in the response analysis. In all 14 patients, tumor size after treatment was determined using CT. Additionally, in 10 patients adequate histologic or cytologic material was obtained through repeated bronchoscopy.

In all patients, T/B had decreased after radiotherapy. An example is shown in Figure 4. The mean T/B decreased from 2.95 ± 0.78 to 1.84 ± 0.29 ($P < 0.001$). With a posttreatment T/B of 1 representing complete disappearance of tumor activity, the average reduction of IMT T/Bs was 52% ± 18%. The data are shown in Figure 5.

Tumor dimensions after radiotherapy, as measured with CT, also diminished significantly in all but one patient. The mean tumor area decreased from 21 ± 14 cm^2 to 7 ± 9 cm^2 ($P < 0.01$), an average reduction of 60% ± 37%. No correlation was found between IMT T/B reduction and tumor size reduction.

Considerable uptake was observed in irradiated normal lung tissue (Fig. 6), with mean R/NR of 1.79 ± 0.53 (range, 1.05–2.27) being significantly different from 1 ($P < 0.001$). The mean uptake ratio between tumors and the adjacent irradiated lung tissue was 1.27 ± 0.34.

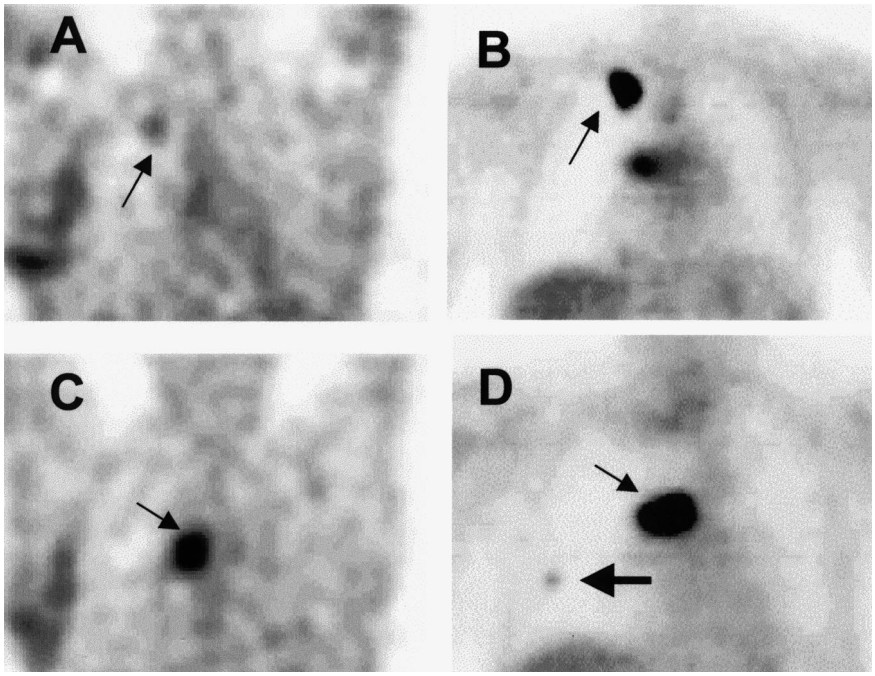

FIGURE 3. IMT SPECT and FDG PET images of patient 1. (A) IMT SPECT coronal slice through 1.5-cm squamous cell lung carcinoma (arrow) in apex of right upper lobe. Nonspecific uptake in lower right chest wall was caused by thoracotomy 20 d earlier. (B) Corresponding FDG PET coronal image, obtained before thoracotomy, shows intense FDG uptake (arrow) in this lesion and hilar metastasis. (C) IMT SPECT coronal slice through hilar region shows intense uptake (arrow) in this large metastasis. (D) Corresponding FDG PET coronal image through middle of this hilar metastasis (small arrow) with higher contrast. Additional lesion in right middle field (large arrow) that was missed on IMT SPECT image was found on PET.

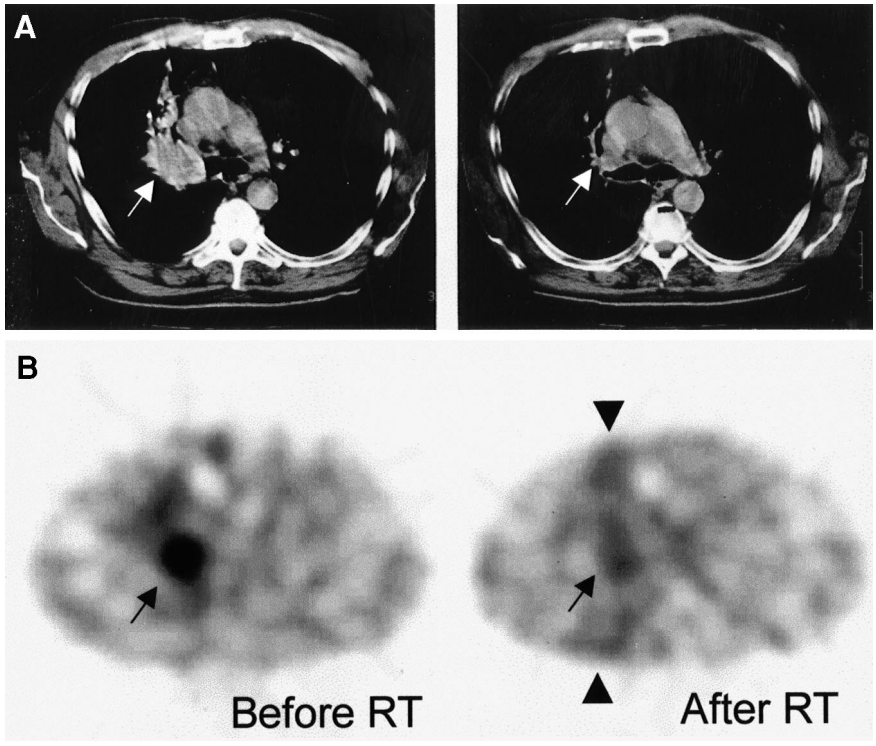

FIGURE 4. Corresponding transverse IMT SPECT (B) and CT (A) slices through squamous cell carcinoma (white arrows) in right upper lobe, before radiotherapy (left) and shortly after (right). CT images show significant tumor regression, but IMT SPECT shows reduced but lightly persisting uptake (black arrows). Viable tumor cells were found after bronchoscopic biopsy. Also note increased uptake in irradiated field (arrowheads).

Biopsies from the tumor area after radiotherapy still contained viable tumor cells in 4 (of 10) patients. The reduction in IMT uptake in these 4 patients was not different from that in patients with negative biopsy findings after radiotherapy, nor was the absolute pre- or posttreatment uptake different (Fig. 5), although the number of studied patients was low. Also, in patients with and without mediastinal metastases, IMT T/Bs before and after radiotherapy were not different.

Third IMT SPECT (Follow-Up)

Three months after the second IMT scan, 13 patients underwent a third IMT SPECT scan. One patient had died

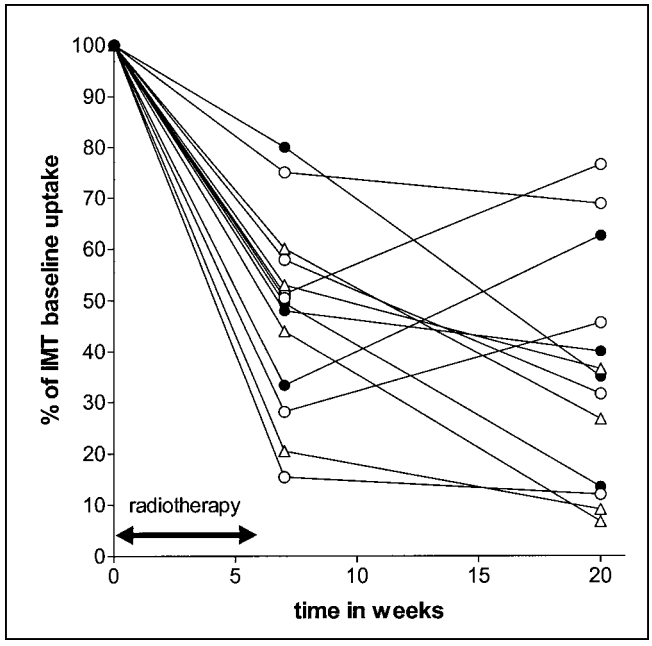

FIGURE 5. IMT T/Bs shortly after radiotherapy and 3 mo later, given as percentage of T/B before radiotherapy. Circles denote patients with (●) or without (○) residual tumor, based on bronchoscopic biopsy shortly after radiotherapy. △ = patients without biopsy.

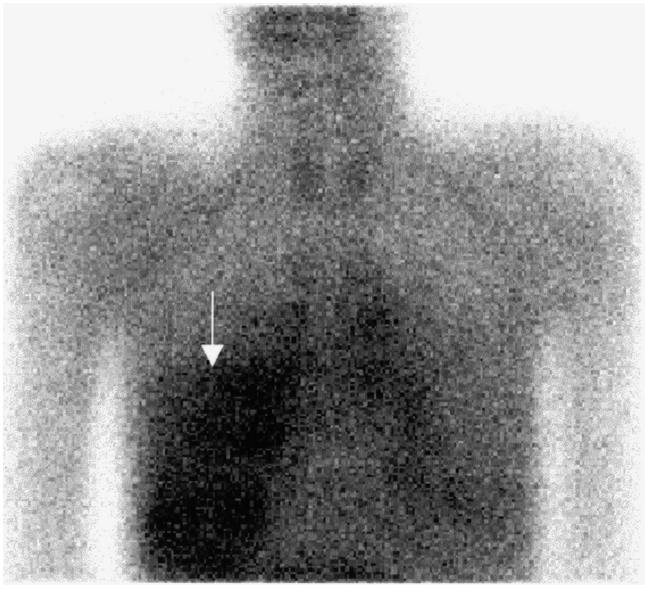

FIGURE 6. Planar IMT image obtained 1 wk after 60 Gy radiotherapy was applied to tumor on right middle lobe of patient 2 (Fig. 1). Increased uptake is present in entire irradiated field (arrow). Diaphragm is at very bottom of image.

between the second and third studies. The mean T/B had decreased slightly from 1.84 ± 0.29 to 1.61 ± 0.41, but this change between the second and third scans was not significant. Only in 1 of the 4 patients with positive biopsy findings, but also in 2 patients with negative biopsy findings after radiotherapy, had T/Bs risen again.

At the end of the follow-up period, 6 patients were still alive; all others had died from their lung cancer. Median survival was 20 mo. Cox regression analysis showed no significant relationship between survival and IMT T/B before or after radiotherapy (relative risk, 0.9, with a wide 95% confidence interval of 0.45–1.8), but more observations are required to study this relationship.

Average R/NR had decreased from 1.79 ± 0.53 to 1.50 ± 0.50, which was a significant difference ($P < 0.05$) but still much higher than 1 ($P < 0.001$). The tumor-to-irradiated lung tissue ratio was 1.21 ± 0.31, which was not different from the ratio after the second study.

DISCUSSION

This study showed that non–small cell lung cancer lesions can be visualized using IMT SPECT. Apparently, this simple and potentially widely available SPECT method is able to reveal the increased amino acid metabolism in these tumors. This ability has not, to our knowledge, been shown before. However, some serious drawbacks that will limit its clinical applicability were noted. First, although all primary tumors > 1.5 cm were detected, a smaller primary tumor was missed. Second, lesion-based sensitivity for mediastinal metastases was low (65%) and for small lesions (<2 cm) even as low as 42%. Because of this detection limit of 1.5–2 cm, IMT SPECT does not appear helpful in mediastinal staging and will not reduce the need for invasive staging procedures.

Shortly after radiotherapy, we found a considerable decrease in IMT uptake intensity in the remaining tumor, indicating decreased amino acid metabolism induced by radiotherapy, although the reduction in size in itself may also contribute to the decreased uptake. We did not observe a relationship between the presence of residual viable tumor tissue and IMT uptake or changes in uptake, but this relationship requires further study and a certain degree of sampling error might have influenced it. However, we also did not find a correlation between survival, another outcome parameter, and IMT uptake. Furthermore, considerable uptake was found in normal lung tissue that had been included in the irradiated field. This phenomenon was present in nearly all patients shortly after radiotherapy and had scarcely diminished 3 mo later. It was not related to the occurrence of radiation pneumonitis or other radiotherapeutic lung damage. Apparently, tissue changes after radiotherapy (inflammation, fibrosis, apoptosis) are associated with increased amino acid demand, limiting the specificity of IMT for evaluation of the results of radiotherapy. Therefore, it seems unlikely that, even in larger groups, IMT SPECT will have predictive value for evaluating the response of individual patients.

Radiolabeled amino acids have hardly been applied in lung cancer imaging. Because amino acids play a minor role in the metabolism of inflammatory cells, the theoretically better specificity may be advantageous in comparison with FDG (*5–7,15*). A high specificity of 91% was indeed reported in a recent study by Yasukawa et al. (*16*), who retrospectively analyzed ^{11}C-methionine PET for mediastinal staging ($n = 41$). PET correctly revealed 10 of 14 enlarged lymph nodes to be tumor-negative, but intense methionine uptake was also present in many histologically negative lymph nodes, independent of size (*16*). Nettelbladt et al. (*17*) found both FDG and ^{11}C-methionine PET to show positive results in four patients with mediastinal metastases but also found methionine (and FDG) to be taken up in postobstructive pneumonia and in mucous membranes of the carina and proximal main bronchi. Kubota et al. (*18*) could separate a group of patients with early tumor recurrence from a group with late recurrence using L-[methyl-^{11}C]-methionine uptake in a study similar to ours but found CT to be better for predicting ultimate local recurrence. However, the increased amino acid uptake in irradiated lung tissue observed in our study has not been described before.

IMT, as a relatively new metabolic tracer and the only amino acid tracer suitable for SPECT, compares well with other single-photon tracers applied in lung cancer. Using ^{201}Tl, ^{99m}Tc-MIBI, or ^{67}Ga, sensitivities between 50% and 90% have been reported for primary tumor detection, with T/Bs between 2.4 and 3.8 (*19–24*). Few studies have addressed mediastinal staging, but in nearly all of these, sensitivity for small lesions (<1.5 cm) was too low to be clinically helpful and uptake in benign processes frequently decreased specificity (*23–25*). In addition, most authors have reported only patient-based sensitivities, whereas lesion or lymph node station–based sensitivities are usually lower. Although as sensitive as these other SPECT agents, the sensitivity of IMT SPECT is too low to be clinically acceptable. Apparently, amino acid uptake is not high enough to compensate for the limited resolution of SPECT. Therefore, negative scan findings do not rule out the presence of (especially small) metastases, so that invasive staging with mediastinoscopy or surgery is still needed. However, one should realize that CT alone does not perform better than single-photon studies (*26*), as is suggested also in this study using IMT SPECT.

CONCLUSION

SPECT using the radiolabeled amino acid IMT is able to reveal non–small cell lung cancer lesions with a high sensitivity for the primary tumor. However, IMT SPECT appears to have a detection limit of approximately 1.5 cm. For mediastinal staging, this limit results in a sensitivity that is too low to be clinically helpful. Although tumor uptake significantly decreased after radiotherapy, relatively high

and persistent uptake was observed in irradiated normal lung tissue. The specificity of IMT is therefore lower than expected, limiting its application in treatment evaluation.

ACKNOWLEDGMENTS

The authors thank Amersham Cygne, Eindhoven, The Netherlands, for help in supplying ^{123}I, Dr. Eduard L. Mooyaart for revision of CT studies, and the University Hospital Groningen for financial support (project OGAZG9902).

REFERENCES

1. Guhlmann A, Stork M, Kotzerke J, Moog F, Sunder-Plassmann L, Reske SN. Lymph node staging in non-small cell lung cancer: evaluation by ^{18}F-FDG positron emission tomography (PET). *Thorax.* 1997;52:428–441.
2. Bury T, Dowlati A, Paulus P, et al. Whole body fluorine-18 deoxyglucose positron emission tomography in the staging of non-small cell lung cancer. *Eur Respir J.* 1997;10:2529–2534.
3. Steinert HC, Hauser M, Allemann F, et al. Non-small cell lung cancer: nodal staging with FDG PET versus CT with correlative lymph node mapping and sampling. *Radiology.* 1997;202:441–446.
4. Berlangieri SU, Scott AM, Knight SR, et al. F-18 fluorodeoxyglucose positron emission tomography in the non-invasive staging of non-small cell lung cancer. *Eur J Cardiothorac Surg.* 1999;16(suppl 1):S25–S30.
5. Strauss LG. Fluorine-18-deoxyglucose and false-positive results: a major problem in the diagnostics of oncological patients. *Eur J Nucl Med.* 1996;23:1409–1415.
6. Kubota K, Matsuzawa T, Fujiwara T, et al. Differential diagnosis of AH109A tumor and inflammation by radioscintigraphy with L-[methyl-^{11}C]-methionine. *Jpn J Cancer Res.* 1989;80:778–782.
7. Kubota R, Kubota K, Yamada S, et al. Methionine uptake by tumor tissue: a microautoradiographic comparison with FDG. *J Nucl Med.* 1995;36:484–492.
8. Langen KJ, Coenen HH, Roosen N, et al. SPECT studies of brain tumors with L-3-[^{123}I]iodo-alpha-methyl-tyrosine: comparison with PET, [^{124}I]IMT and first clinical results. *J Nucl Med.* 1990;31:281–286.
9. Jager, PL, Franssen EJF, Kool W, et al. Feasibility of tumor imaging using L-3-[^{123}I]iodo-alpha-methyl-tyrosine in extra-cranial tumors. *J Nucl Med.* 1998; 39:1736–1743.
10. Langen KJ, Roosen N, Coenen HH, et al. Brain and brain tumor uptake of L-3-[^{123}I]iodo-alpha-methyl-tyrosine: competition with natural L-amino acids. *J Nucl Med.* 1991;32;1225–1228.
11. Jager PL, de Vries EGE, Piers DA, Timmer-Bosscha H. Uptake mechanisms of L-3-[^{125}I]iodo-alpha-methyl-tyrosine in a human small-cell lung cancer cell line: comparison with L-1-[^{14}C]-tyrosine. *Nucl Med Commun.* 2001:in press.
12. Isselbacher KJ. Sugar and amino acid transport by cells in culture: differences between normal and malignant cells. *N Engl J Med.* 1972;286:929–933.
13. Jager PL, Plaat BEC, de Vries EGE, et al. Imaging of soft-tissue tumors using L-3-[iodine-123]iodo-alpha-methyl-tyrosine SPECT: comparison with proliferative and mitotic activity, cellularity and vascularity. *Clin Cancer Res.* 2000;6: 2252–2259.
14. Kuwert T, Probst-Cousin S, Woesler B, et al. Iodine-123-alpha-methyl tyrosine in gliomas: correlation with cellular density and proliferative activity. *J Nucl Med.* 1997;38:1551–1555.
15. Kubota K, Tada M, Yamada S, et al. Comparison of the distribution of fluorine-18 fluoromisonidazole, deoxyglucose and methionine in tumor tissue. *Eur J Nucl Med.* 1999;26:750–757.
16. Yasukawa T, Yoshikawa K, Aoyagi H, et al. Usefulness of PET with ^{11}C-methionine for the detection of hilar and mediastinal lymph node metastasis in lung cancer. *J Nucl Med.* 2000;41:283–290.
17. Nettelbladt OS, Sundin AE, Valind SO, et al. Combined fluorine-18-FDG and carbon-11-methionine PET for diagnosis of tumors in lung and mediastinum. *J Nucl Med.* 1998;39:640–647.
18. Kubota K, Yamada S, Ishiwata K, et al. Evaluation of treatment response of lung cancer with positron emission tomography and L-[methyl-^{11}C]methionine: a preliminary study. *Eur J Nucl Med.* 1993;20:495–501.
19. Higashi K, Nishikawa, Seki H, et al. Comparison of fluorine-18-FDG PET and thallium-201 SPECT in evaluation of lung cancer. *J Nucl Med.* 1998;38:9–15.
20. Ragheb AM, Elgazzar AHH, Ibrahim AK, et al. A comparative study between planar Ga-67, Tl-201 images, chest x-ray and x-ray CT in inoperable non-small cell carcinoma of the lung. *Clin Nucl Med.* 1995;20:426–433.
21. Matsuno S, Tanabe M, Kawasaki Y, et al. Effectiveness of planar image and single photon emission tomography of thallium-201 compared with gallium-67 in patients with primary lung cancer. *Eur J Nucl Med.* 1992;19:86–95.
22. Nishiyama Y, Kawasaki Y, Yamamoto Y, et al. Technetium-99m-MIBI and thallium-201 scintigraphy in primary lung cancer. *J Nucl Med.* 1997;38:1358–1361.
23. Chiti A, Maffioli LS, Inffante M, et al. Assessment of mediastinal involvement in lung cancer with technetium-99m-sestamibi SPECT. *J Nucl Med.* 1996;37:938–942.
24. Kashitani N, Makihara S, Maeda T, Eda T, Takeyama H, Hiraki Y. Thallium-201-chloride and technetium-99m-MIBI SPECT of primary and metastatic lung carcinoma. *Oncol Rep.* 1999;6:127–133.
25. Abdel-Dayem HM, Scott A, Macapinlac H, Larson S. Tracer imaging in lung cancer. *Eur J Nucl Med.* 1994;21:57–81.
26. Yokoi K, Okuyama A, Mori K, et al. Mediastinal lymph node metastasis from lung cancer: evaluation with Tl-210 SPECT—comparison with CT. *Radiology.* 1994;192:813–817.